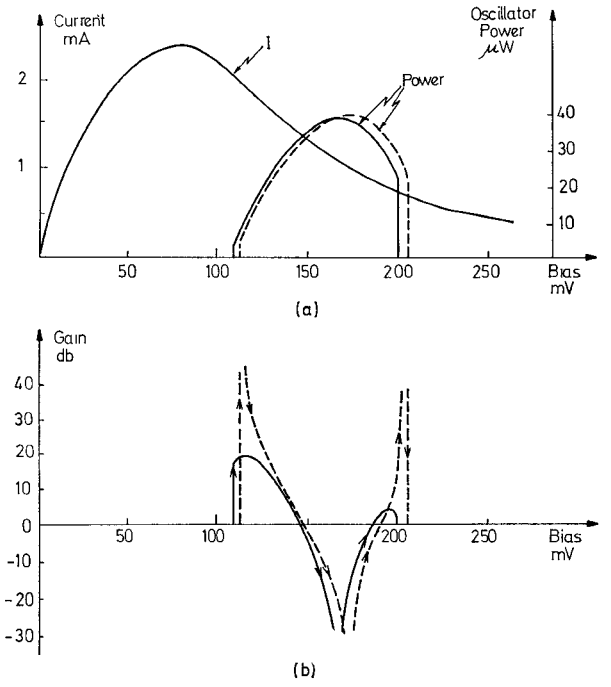

Fig. 3. (a) I–V characteristics of Microwave Associates tunnel-diode MA4605B. Superimposed on it is the self-oscillation power. (b) Variation of conversion gain with applied bias. Solid lines represent the result when maximum gain is adjusted to 20 dB; broken lines represent the results when the mixer is adjusted to give oscillations.

Experimental Results

Fig. 3(a) shows the diode I–V characteristics of Microwave Associates type MA4605B, and superimposed on it is the self-oscillation power dissipated in the source resistance (50 Ω). Fig. 3(b) shows the variations of gain with respect to bias; the effect of the voltage-dependent depletion-layer capacitance on the self-oscillation frequency is taken into account by retuning at each applied bias.

As will be seen, the maximum oscillation power region corresponds to the minimum conversion gain (a loss of more than 30 dB). This is also observable in the broken line case where the bias point for both the maximum oscillation power and the minimum gain positions shift slightly. The experiments are repeated with two other tunnel diodes differing in characteristics and exactly the same conditions are obtained. The positive gain regions in the two different bias regions correspond more or less to the same oscillation power level.

The difference in gains for small and large oscillator magnitudes has been calculated by Barber [7]. Large critical gain with low self-oscillation power coincides with Barber's results; however, the high losses encountered in the case of self-oscillations having large magnitude cannot be explained by Barber's results. The origin of this anomalous behavior is not yet understood.

The image rejection of the mixer was about 15 dB independent of all gain conditions, and the noise figure for positive gains was 6 dB. Fig. 4 shows the linearity of the self-oscillating tunnel-diode mixer for different gain conditions.

Conclusions

In view of the techniques used, it is feasible to extend the operating frequencies into the higher microwave region.

The measured noise figure of the mixer is higher than those reported previously. This is partly due to the sliding contact resistances and the losses occuring in the lumped elements, and is partly due to the source impedance which is not optimized. The latter is not curable because the source impedance has to be of the order of the negative resistance of the tunnel diode at the operating bias to cause oscillation.

The sharp and well-defined dependency of the minimum gain on the peak of the oscillation magnitude suggests that some correlation

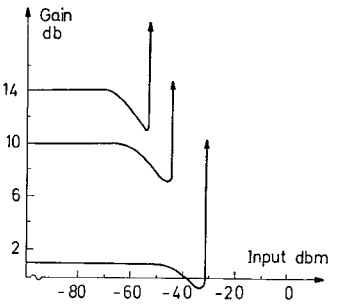

Fig. 4. Conversion gain as a function of input signal power. Steep lines with the arrow heads represent oscillations.

exists between the maximum oscillation magnitude and the available conversion gain. An explanation without a proof may be that at this bias point, all the available RF power from the tunnel diode occurs at the oscillation frequency and, consequently, the power output at any other frequency is largely minimized.

References

[1] K. K. N. Chang, G. H. Heilmeier, and H. J. Prager, "Low-noise tunnel-diode down converter having conversion gain," *Proc. IRE*, vol. 48, pp. 854–858, May 1960.
[2] W. A. Gambling and S. Basu Mallick, "Tunnel-diode mixers," *Proc. Inst. Elec. Eng.*, vol. 112, no. 7, pp. 1311–1318, July 1965.
[3] J. O. Scanlan, *Analysis and Synthesis of Tunnel-Diode Circuits*. New York: Wiley, 1965, ch. 5, p. 252.
[4] G. L. Alley and K. W. Atwook, *Electronic Engineering*. New York: Wiley, 1966, ch. 14, p. 563.
[5] R. D. Gallagher, "A microwave tunnel-diode amplifier," *Microwave J.*, vol. 8, no. 2, p. 62, Feb. 1965.
[6] H. J. Reich, "The growth of oscillations in two-resonator negative-conductance oscillators," *IEEE Trans. Circuit Theory*, vol. CT-15, pp. 259–262, Sept. 1968.
[7] M. R. Barber, "A numerical analysis of the tunnel-diode frequency converter," *IEEE Trans. Microwave Theory Tech.* (*Special Issue on Microwave Filters*), vol. MTT-13, pp. 663–670, Sept. 1965.

P-I-N Variable Attenuator with Low Phase Shift

W. J. PARRIS

***Abstract*—A broad-band MIC current-controlled variable attenuator that exhibits small phase change versus attenuation has been developed. Design factors that effect phase shift are discussed. Performance at frequencies between 0.5 and 3.0 GHz is shown.**

Measured values of attenuation are shown to be independent of frequency from 0.5 to 3.0 GHz.

The development of solid-state radar systems using electronically steerable array-type antennas has generated the need for electronically variable microwave-integrated-circuit attenuators that display minimum phase change versus attenuation. These attenuators must also be impedance matched at both the input and the output terminals. This short paper describes the problems encountered and the solutions devised to produce a minimum phase change versus attenuation impedance-matched electronically variable attenuator.

To meet the requirement that the input and output impedances remain constant with changing attenuation, it is necessary to provide three variable elements in a passive attenuator. This is readily realized with the conventional tee- or pi-section resistive attenuator. A handy form of the variable resistor at microwave frequencies is the p-i-n diode. For the present project, silicon p-i-n diodes[1] in chip form were selected and evaluated in terms of microwave impedance versus forward current.

Manuscript received October 8, 1971; revised April 13, 1972. This work was supported in part by the Naval Air Systems Command under Contract N00019-70-C-0584.

The author is with the Westinghouse Defense and Electronic Systems Center, Baltimore, Md. 21203.

[1] Type DSC-6157-99 from Alpha Industries, Woburn, Mass.

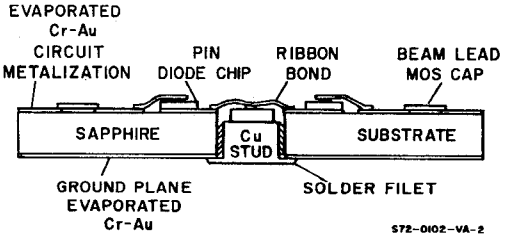

Fig. 1. Cross-section sketch showing construction features.

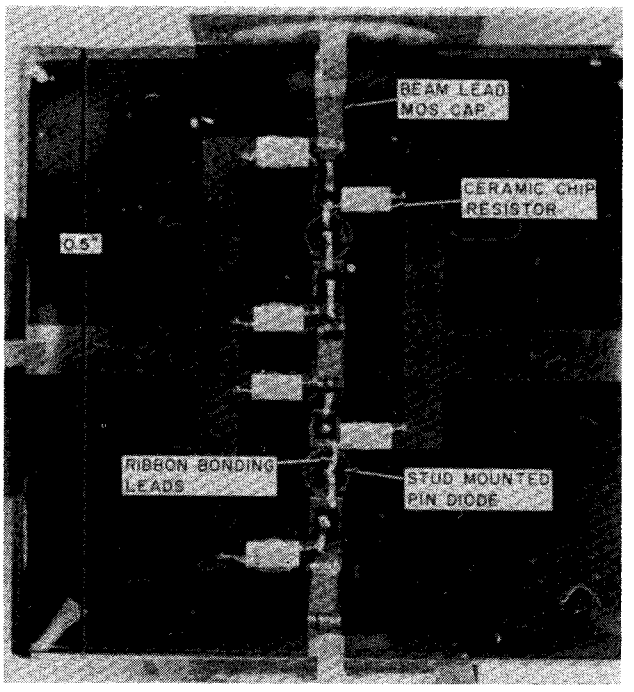

Fig. 2. Parts layout.

For the desired attenuation range of 25 dB with a minimum attenuation of 5 dB, a single tee section would require resistance values in the shunt arm varying from a low of 3.165 Ω to a maximum of 82.24 Ω. To avoid the low value of resistance which would compete in magnitude with the reactance of the approximately 0.3-nH bonding lead and circuit inductance, a two-stage attenuator was designed with two tee sections in series. The resistance range required in this case is 7.14–167 Ω. The larger value of resistance is still small enough not to be seriously shunted by the junction capacitance of the diode.

The circuit was initially designed with bias blocking capacitors in the shunt arm to allow a single variable voltage to control attenuation. The resulting 80°–90° phase change versus attenuation at 1.0 GHz was traced to the transmission line reactance of the shunt arm which was 0.06 guide wavelength long.

As shown in Figs. 1 and 2, a new layout was devised in which the shunt diodes are directly grounded by means of metal posts extending through the substrate to contact the ground plane. This new arrangement calls for a bias circuit that has two variable currents to control the resistance of the p-i-n diodes, as shown in the accompanying schematic Fig. 3. A particular feature of this layout is that the bonding leads for the shunt diodes now appear in the series RF path where the effect on phase is less pronounced. The use of ribbon leads 5 mil wide for contacting the diodes further reduces inductive effects. Beam lead capacitors[2] were used for their small size and inherent low inductance. The ceramic chip resistors[3] were selected for small size.

As is to be expected, the inductance in series branch of the tee produces some phase change versus attenuation, with this change

[2] Type SC-90010M from Alpha Industries, Woburn, Mass.
[3] Type 2C102J from Film Microelectronics, Inc. (FMI), Burlington, Mass.

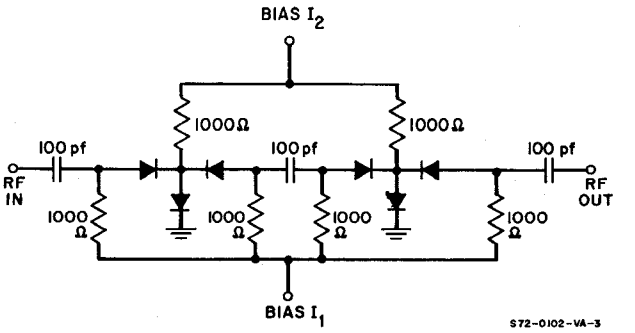

Fig. 3. Attenuator circuit schematic.

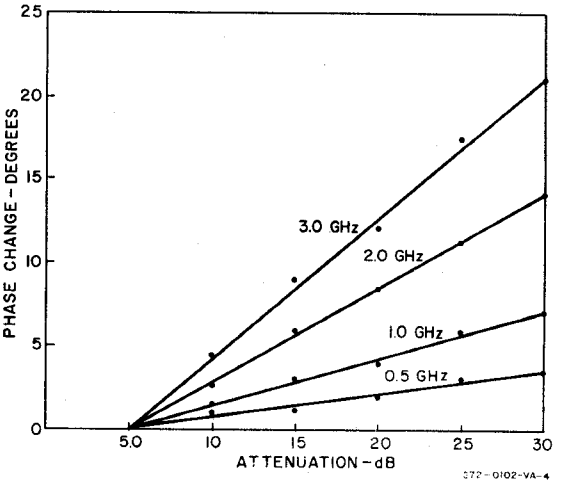

Fig. 4. Phase-shift variation versus attenuation.

increasing with increasing frequency. This effect is shown in Fig. 4 on the plot of phase change versus attenuation, for frequencies between 0.5 and 3.0 GHz.

The impedance match of the attenuator is excellent since the independent control currents can be adjusted for best match at a given attenuation setting. With the control currents adjusted at 1.0 GHz, the impedance match at 0.5 GHz and at 3.0 GHz is better than 1.3:1 for the full range of attenuation.

The efforts on behalf of achieving minimum phase change versus attenuation have provided a bonus in the form of wide-band operation. Attenuation versus frequency shows less than ±0.5-dB change of attenuation over a frequency range of 0.5–3.0 GHz when the two control currents are adjusted at 1.0 GHz. Further measurements are in progress to determine the upper and lower frequencies at which rolloff begins.

Conclusions

In lumped-element microwave circuitry it is not always sufficient to specify that individual components be dimensionally small in terms of wavelength. In sensitive branches of circuits it is necessary that the entire string of components and their mounting pads be considered and the effective transmission line length of the branch be included in the calculations.

In the electrically variable attenuator described above the change in transmission phase versus attenuation was reduced by a factor of 10 through application of this principle.

Improved high-frequency performance could be obtained through the use of beam lead diodes in the series branch to reduce chip size and bonding lead inductance.

Acknowledgment

The author wishes to thank D. W. Maki for his assistance with the computer analysis portions of this program.

Exact Design of Stepped-Impedance Transformers

FENG-CHENG CHANG AND HAROLD MOTT

***Abstract*—The exact solutions of the design of stepped-impedance transformers presented until now have been tedious and subject to computational error. We present here an exact synthesis procedure which requires less effort than other exact procedures. In addition, two recurrence formulas are given for determining the characteristic impedances of each section. The coefficients so obtained can be compared to eliminate computational errors.**

Stepped-impedance transformers (SIT's) have been discussed frequently in the literature. Exact [1]–[3], approximate [4], and graphical solutions [5], as well as design tables [3], [6], have been published. The exact solutions published thus far are tedious and susceptible to computational error. In this short paper we present an exact synthesis procedure which can be carried out with less effort than is necessary with some other procedures.

The SIT consists of n lossless transmission-line sections, each of electrical length ϕ, terminated in resistive loads R_g and R_L. The input impedance of the r section, looking to the left, is

$$Z_{\text{in},r}(\phi) = Z_r \frac{Z_{\text{in},r-1}(\phi) + jZ_r \tan\phi}{Z_r + jZ_{\text{in},r-1}(\phi)\tan\phi} \tag{1}$$

where $Z_{\text{in},r-1}(\phi)$ is the input impedance of the $(r-1)$ section and Z_r is the characteristic impedance of the r section.

If we introduce the frequency variable $s = j\tan\phi$ [1] and define

$$z_r(s) = \frac{Z_{\text{in},r}(s)}{Z_{r+1}} \tag{2}$$

$$\zeta_r = \frac{Z_r}{Z_{r+1}} \tag{3}$$

we may write a normalized form of (1) as

$$z_r(s) = \zeta_r \frac{z_{r-1}(s) + s}{1 + z_{r-1}(s)s} \tag{4}$$

from which we note that

$$\zeta_r = z_r(1) = -z_r(-1). \tag{5}$$

In these equations, $r = 1, 2, \cdots, n$, $Z_{n+1} = R_L$, $Z_0 = R_g$, and $R = R_L/R_g = Z_{n+1}/Z_0$. We may solve (4) to obtain

$$z_{r-1}(s) = \frac{\zeta_r s - z_r(s)}{z_r(s)s - \zeta_r}. \tag{6}$$

If we know $z_n(s)$, we see from (5) and (6) that we may find $z_r(s)$ and ζ_r for all r. Further, from a knowledge of $Z_{n+1}(=R_L)$, (3) may be used successively to find the characteristic impedances Z_r of all sections of the SIT.

The direct use of (6) to determine the normalized impedance functions is not convenient, and we will develop a more convenient method. For a lossless SIT we may express $z_r(s)$ as

$$z_r(s) = \sum_{k=0}^{r} N_k{}^r s^k \Big/ \sum_{k=0}^{r} M_k{}^r s^k. \tag{7}$$

We substitute (7) into (6), which becomes

$$z_{r-1}(s) = \sum_{k=0}^{r+1} (\zeta_r M_{k-1}{}^r - N_k{}^r)s^k \Big/ \sum_{k=0}^{r+1} (N_{k-1} - \zeta_r M_k{}^r)s^k \tag{8}$$

if we note that $M_{-1}{}^r = N_{-1}{}^r = M_{r+1}{}^r = N_{r+1}{}^r = 0$.

Manuscript received October 18, 1971, revised January 7, 1972.
The authors are with the Electrical Engineering Department, University of Alabama, University, Ala. 35486.

From (8), $z_{r-1}(s)$ appears at first to contain polynomials of higher order than $z_r(s)$. However, if we substitute $s = \pm 1$ into (6) and use (5), we see that both numerator and denominator are zero. Thus the factor (s^2-1) may be removed from both numerator and denominator of $z_{r-1}(s)$.

Let us write $z_{r-1}(s)$ as

$$z_{r-1}(s) = \sum_{k=0}^{r-1} N_k{}^{r-1} s^k \Big/ \sum_{k=0}^{r-1} M_k{}^{r-1} s^k \tag{9}$$

where we wish to determine the coefficients $M_k{}^{r-1}$ and $N_k{}^{r-1}$ from the known coefficients $M_k{}^r$ and $N_k{}^r$. We multiply the numerator and denominator of (9) by (s^2-1) and compare the result to (8), and obtain

$$N_{k-2}{}^{r-1} - N_k{}^{r-1} = \zeta_r M_{k-1}{}^r - N_k{}^r \tag{10a}$$

$$M_{k-2}{}^{r-1} - M_k{}^{r-1} = N_{k-1}{}^r - \zeta_r M_k{}^r. \tag{10b}$$

These equations may be solved to give

$$N_k{}^{r-1} = (N_k{}^r + N_{k-2}{}^r + N_{k-4}{}^r + \cdots) - \zeta_r(M_{k-1}{}^r + M_{k-3}{}^r + M_{k-5}{}^r + \cdots) \tag{11a}$$

$$M_k{}^{r-1} = \zeta_r(M_k{}^r + M_{k-2}{}^r + M_{k-4}{}^r + \cdots) - (N_{k-1}{}^r + N_{k-3}{}^r + N_{k-5}{}^r + \cdots) \tag{11b}$$

where the series are continued over positive subscripts only, in accord with our statement following (8). We may also obtain from (10) a different form,

$$N_k{}^{r-1} = \zeta_r(M_{k+1}{}^r + M_{k+3}{}^r + M_{k+5}{}^r + \cdots) - (N_{k+2}{}^r + N_{k+4}{}^r + N_{k+6}{}^r + \cdots) \tag{12a}$$

$$M_k{}^{r-1} = (N_{k+1}{}^r + N_{k+3}{}^r + N_{k+5}{}^r + \cdots) - \zeta_r(M_{k+2}{}^r + M_{k+4}{}^r + M_{k+6}{}^r + \cdots) \tag{12b}$$

with the series continued only for subscripts less than or equal to superscripts.

From (11) we may obtain the compact recurrence relations

$$N_k{}^{r-1} = N_k{}^r - M_{k-1}{}^{r-1} \tag{13a}$$

$$M_k{}^{r-1} = \zeta_r M_k{}^r - N_{k-1}{}^{r-1} \tag{13b}$$

and from (12) we get

$$N_k{}^{r-1} = \zeta_r M_{k+1}{}^r - M_{k+1}{}^{r-1} \tag{14a}$$

$$M_k{}^{r-1} = N_{k+1}{}^r - N_{k+1}{}^{r-1}. \tag{14b}$$

Equations (13) or (14)—or alternatively (11) or (12)—may be used to reduce the order of the normalized impedance function each time they are applied. Thus, by their use, if $z_n(s)$ is given, all of the n characteristic impedances of the SIT may be found. Note that if (11) or (13) is used, we find a coefficient in terms of the coefficients of equal and lower powers of s, whereas, (12) or (14) gives a coefficient in terms of the coefficients of equal and higher powers of s. This gives us a highly useful check on computational errors in determining the coefficients.

In general the power reflection coefficient for a lossless n-section SIT may be written as [4]

$$|\rho(\phi)|^2 = \frac{L_{2n}(\cos\phi)}{1 + L_{2n}(\cos\phi)} \tag{15}$$

where $L_{2n}(\cos\phi)$ is an even polynomial of degree $2n$. By the transformation $s = j\tan\phi$ we may write the voltage reflection coefficient and the input impedance function as

$$\rho(s) = \frac{Q_n(s)}{P_n(s)} \tag{16}$$

$$z_n(s) = \frac{P_n(s) + Q_n(s)}{P_n(s) - Q_n(s)} \tag{17}$$